Preparation of rare earth two-dimensional nano-thin film using PET as carrier

Jiaxin Wang[1], Junwei Li[1] ✉, Min Zhang[2] ✉, Baohang Zhang[1], Zhehui Li[1], Yuting Wang[1], Yulong Wu[1], Qianjin Zhang[1], Wanxiang Yao[1]

[1]*School of Materials Science and Engineering, Tianjin Chengjian University, Tianjin 300384, People's Republic of China*
[2]*Department of Scientific Research, Logistics University of Chinese People's Armed Police Forces, Tianjin 300309, People's Republic of China*
✉ *E-mail: lijunwei2001@tcu.edu.cn; 1525944192@qq.com*

Published in Micro & Nano Letters; Received on 27th July 2017; Revised on 23rd October 2017; Accepted on 10th November 2017

A structurally ordered rare earth two-dimensional nano-thin film using polyethylene terephthalate (PET) as carrier was obtained using the homogeneous precipitation method. Films with different sizes and morphologies were prepared by adjusting reaction temperature, reaction time and concentration of reactant. Microstructures of the films were obtained by scanning electron microscopy and energy dispersive spectrometry, and the results showed that the sample revealed the optimal micro-morphology when it was prepared at 85°C for 24 h with the concentration of $Y(NO_3)_3.6H_2O$, H_2NCONH_2 and $C_{12}H_{25}SO_4Na$ fixed at 0.01 M, 0.04 M and 7 g/l, respectively. Moreover, uniform, dense and ordered films were successfully prepared over a large area at the gas–liquid surface using PET as carrier.

1. Introduction: Rare earth ions have been found to be versatile as key materials for fluorescence, magnetic, electronic, catalysts, laser and ceramic material applications [1–6]. In recent years, rare earth two-dimensional thin films have been widely used in various fields. Preparation methods of rare earth two-dimensional thin film materials mainly include the hydrothermal synthesis method, the homogeneous precipitation method and the ion exchange method [7–9].

The hydrothermal synthesis method is characterised by high particle purity and good dispersion, but equipment requirements are demanding, the technical difficulty is large and the safety performance is poor. Although the ion exchange method is simple, operation is much more complicated. Compared with above two preparation methods, the homogeneous precipitation method [10–12] is simple to operate, and the particle growth rate can be controlled within an appropriate range, so as to obtain well-balanced particle size, and high purity nanoparticles, which makes it more conducive to industrial production. Due to these advantages, Borlaf *et al.*[13] prepared rare earth-doped TiO_2 nanocrystalline thin films by the homogeneous precipitation method.

In summary, in view of the reported morphological imperfection problems in thin films, we use a simple homogeneous precipitation method to prepare a uniform, dense, ordered and large-scale growth of rare earth two-dimensional nano-thin film. Polyethylene terephthalate (PET) thin film is a colourless, odourless, transparent and shiny thin film with good mechanical and optical properties, chemical resistance and moderate biocompatibility [14–16]. Therefore, we use it as a carrier for the thin film.

2. Experimental

2.1. Materials: Using analytically pure yttrium trinitrate hexahydrate ($Y(NO_3)_3 6H_2O$) and urea (H_2NCONH_2) as raw materials, sodium dodecyl sulphate ($C_{12}H_{25}SO_4Na$) as surfactant, and deionised water as solvent, PET sheet was used as a carrier for thin film growth.

2.2. Preparation of yttria thin film: The $Y(NO_3)_3 6H_2O$, H_2NCONH_2 and $C_{12}H_{25}SO_4Na$ were dissolved in 20 ml deionised water, using ultrasonic agitation until complete dissolution. The surface-treated PET carrier was placed on the gas–liquid surface of the reaction vessel containing the mixed solution, and reacted at a constant temperature to prepare a rare earth oxide thin film.

2.3. Characterisation of yttria thin film: Morphologies of samples were studied using a PHILIPS XL-30 scanning electron microscope (SEM) operated at an accelerating voltage of 5 kV, gold was surface coated for SEM measurement.

3. Results and discussion: The SEM was used to characterise the morphology of the sample prepared at 85°C for 24 h with concentration of $Y(NO_3)_3 6H_2O$, H_2NCONH_2 and $C_{12}H_{25}SO_4Na$ fixed at 0.01 M, 0.04 M and 7 g/l, respectively. Fig. 1*a* shows typical SEM images of rare earth oxide nano-thin film using PET as carrier, which we could see a uniform, dense, ordered and large-scale growth of two-dimensional nano-thin film formed by tightly connected nanowires. The energy dispersive spectroscopy (EDS) element analysis results (elemental distribution for Y and O shown in Fig. 1*b*) confirmed that the sample was Y_2O_3.

The effect of three factors was evaluated: reactant concentration, reaction temperature and reaction time on the microstructure of rare earth oxide nano-thin film using PET as carrier. The series of SEM micrographs in Fig. 2 presents the effect of reactant concentration on the shape and size of products. All other experimental conditions, such as the concentration of surfactant, reaction temperature and reaction time, were all fixed as indicated by the optimum conditions. It can be seen from Fig. 2 that the concentration of $Y(NO_3)_3 6H_2O$ 0.01 M gave the best morphology and the most extensive coverage. Fig. 2*a* shows the morphology of the as-prepared samples, which was rod-shaped partially assembled together and scattered. As illustrated in Fig. 2*b*, the diameter and the length of the rod-like products were 300 and 800 nm, respectively. The sample coverage was higher than that of Fig. 2*a*, but it was still assembled and disordered. Fig. 2*d* shows that disordered nanorods form thin films with partial deposits. As the precipitate particles growing in the solution had supersaturation, when the concentration of reactants increased, the precipitate particles gathered together, it was difficult to form a dense and orderly thin film.

The rate of product precipitation critically depended on reaction temperature. To quantify this effect, reaction temperature was varied between 75 and 90°C. Other experimental conditions were kept constant. It showed that 85°C was the optimum. The morphology, size and distribution of the products at 85°C were the best (Fig. 3*c*). When the reaction temperature was 75°C (Fig. 3*a*), the products were nanorods with diameter and length of 200 and 500 nm, respectively. Since some of them were irregularly

doi: 10.1049/mnl.2017.0570

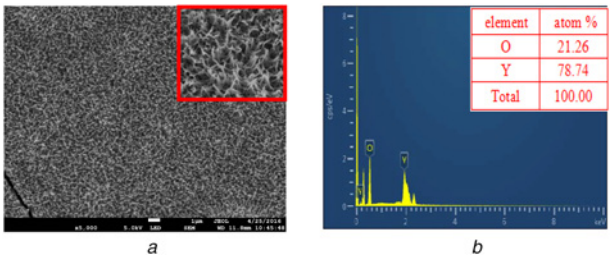

Fig. 1 *SEM and EDS images of rare earth oxide nano-thin film using PET as carrier*
a SEM image
b EDS image

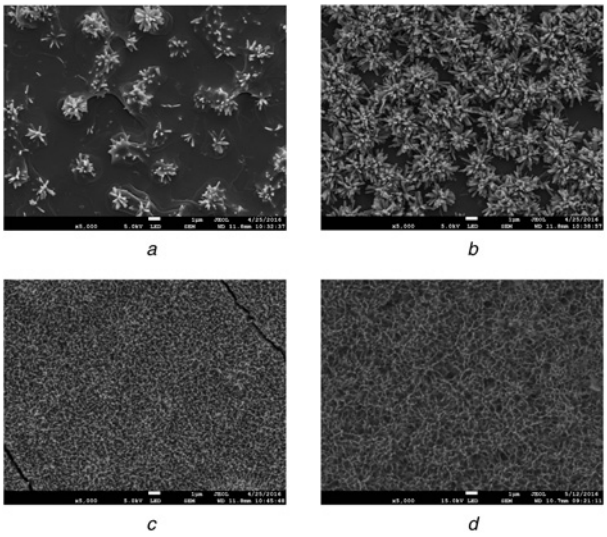

Fig. 2 *SEM images of rare earth oxide nano-thin film using PET as carrier prepared in different concentrations of reactant*
a $Y(NO_3).6H_2O$ 0.001 M, H_2NCONH_2 0.004 M
b $Y(NO_3).6H_2O$ 0.002 M, H_2NCONH_2 0.008 M
c $Y(NO_3).6H_2O$ 0.01 M, H_2NCONH_2 0.04 M
d $Y(NO_3).6H_2O$ 0.02 M, H_2NCONH_2 0.08 M

assembled together, the thin film could not be formed. At 80°C (Fig. 3*b*), the products were assembled disorderly by nanorods with a diameter of about 100 nm, although the coverage was higher than at 75°C without forming a thin film. When the reaction temperature was too high, the hydrolysis rate of the homogeneous precipitant urea was too fast, resulting in deposits that destroy the orderly and dense thin film (Fig. 3*d*).

Furthermore, reaction time also greatly affected the morphology of the samples. Under 85°C and fixed concentration of Y $(NO_3)_3 6H_2O$, H_2NCONH_2 and $C_{12}H_{25}SO_4Na$ at 0.01 M, 0.04 M and 7 g/l, respectively, the reaction time ranged from 12 to 72 h, and their SEM images are shown in Fig. 4. It can be seen from the figure that the reaction time had no regular change in the formation of the thin film, but it had a great influence on the regularity of the thin film formation, and the optimum reaction time was 24 h (Fig. 4*b*). As shown in Fig. 4*a*, the nanorods with a diameter of 100 nm were disordered so that a uniform thin film could not be formed. Fig. 4*c* demonstrates that when the reaction time was 48 h, because of the release of excess hydroxide ions, the product essentially was a sediment without regular morphology. When the reaction time was further extended to 72 h (Fig. 4*d*), due to the reaction time, secondary growth might occur, resulting in the emergence of hole structure.

Based on the above observation, the reaction mechanism of the rare earth oxide nano-thin film prepared by the homogeneous precipitation method using PET as the carrier included two distinct steps: (i) hydrolysis of H_2NCONH_2 (1) and (ii) precipitation reaction (2)

$$(NH_2)_2CO + 3H_2O = 2NH_4^+ + 2OH^- + CO_2 \quad (1)$$

$$2Y^{3+} + 3OH^- = Y_2O_3 + 3H^+ \quad (2)$$

In the above steps, (2) is an instantaneous reaction, and (1) is a slow reaction, which is a step in controlling the reaction rate. Fig. 5 shows a possible schematic representation of the transformation from the disordered nanorods into the large area thin film formed by ordered connected nanowires. It can be seen from the figure that with the increase of the reactant concentration, the reaction temperature and the reaction time, the rod-like product may gradually change from monodisperse stubby form to partially assemble

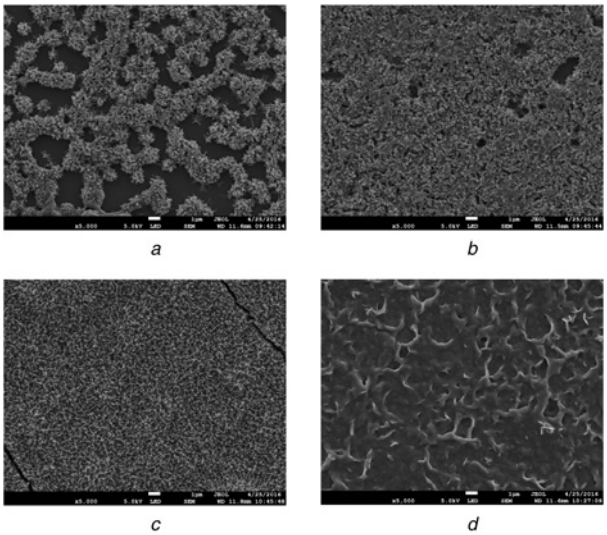

Fig. 3 *SEM images of rare earth oxide nano-thin film using PET as carrier prepared in different reaction temperatures*
a 75°C
b 80°C
c 85°C
d 90°C

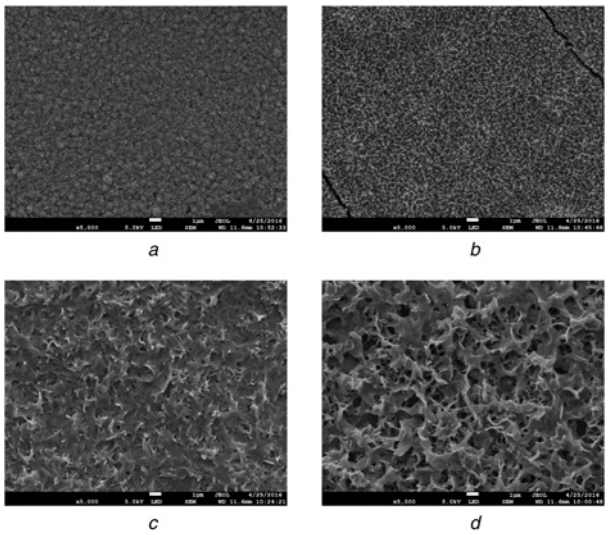

Fig. 4 *SEM images of rare earth oxide nano-thin film using PET as carrier prepared in different reaction times*
a 12 h
b 24 h
c 48 h
d 72 h

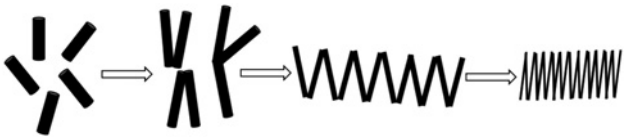

Fig. 5 *Schematic representation of rare earth oxide nano-thin film growth process using PET as carrier*

together in a slender shape. When the three factors reach the appropriate conditions, the product changed into a uniform and dense thin film formed by tightly connected nanowires.

4. Conclusion: Rare earth oxide two-dimensional nano-thin film was successfully prepared at the gas–liquid surface using PET as carrier by the homogeneous precipitation method. The preparation conditions of the samples including reactant concentration, reaction temperature and reaction time were optimised by the SEM images of the samples. Based on this, we conclude as follows: when the sample was prepared at 85°C for 24 h with the concentration of $Y(NO_3)_36H_2O$, H_2NCONH_2 and $C_{12}H_{25}SO_4Na$ fixed at 0.01 M, 0.04 M and 7 g/l, respectively, it shows a uniform, dense, ordered and large-scale growth of rare earth oxide two-dimensional nano-thin film.

5. Acknowledgments: This work was supported by the National Natural Science Foundation of China (grant no. 51508372) and Natural Science Foundation of Tianjin (grant no. 15JCYBJC28600).

6 References

[1] Dai P., Sun Y., Bao Z., *ET AL.*: 'Optical and adsorption properties of mesoporous $SiO_2/Zn_2SiO_4:Eu^{3+}$ hollow nanospheres', *Micro Nano Lett.*, 2017, **12**, (4), pp. 248–251

[2] Zhuang J.Q., Sun Q.J., Zhou Y., *ET AL.*: 'Solution-processed rare-earth oxide thin films for alternative gate dielectric application', *ACS Appl. Mater. Interfaces*, 2016, **8**, (45), pp. 31128–31135

[3] Tomar R., Kumar P., Kumar A., *ET AL.*: 'Investigations on structural and magnetic properties of Mn doped Er_2O_3', *Solid State Sci.*., 2017, **67**, pp. 8–12

[4] Pravinraj S., Vijayakumar M., Marimuthu K.: 'Enhanced luminescence behaviour of Eu^{3+} doped heavy metal oxide telluroborate glasses for laser and LED applications', *Physica B*, 2017, **509**, pp. 84–93

[5] Zhang P.X., Chen Z.Q., Hang Y., *ET AL.*: 'Enhanced emission of the 1.50–1.67 mm fluorescence in Er^{3+}, Ce^{3+}-codoped $Lu_3Al_5O_{12}$ crystal', *J. Alloys Compd.*, 2017, **696**, pp. 795–798

[6] Kulah E., Marot L., Steiner R., *ET AL.*: 'Surface chemistry of rare-earth oxide surfaces at ambient conditions: reactions with water and hydrocarbons', *Sci. Rep.*, 2017, **7**, pp. 1–10

[7] Li Z.Q., Wang W.J., Zhao Z.C., *ET AL.*: 'One-step hydrothermal preparation of Ce-doped MoO_3 nanobelts with enhanced gas sensing properties', *RSC Adv.*, 2017, **7**, (45), pp. 28366–28372

[8] Abu-Zied B.M., Hussein M.A., Asiri A.M., *ET AL.*: 'Synthesis, characterization and electrical conductivity of nano-crystalline erbium sesquioxideby the precipitation method and subsequent calcination', *Int. J. Electrochem. Sci.*, 2016, **11**, pp. 7182–7197

[9] Kreek K., Kriis K., Maaten B., *ET AL.*: 'Organic and carbon aerogels containing rare-earth metals: their properties and application as catalysts', *J. Non-Cryst. Solids*, 2014, **404**, pp. 43–48

[10] Jiang X.L., Du Y., Wang W., *ET AL.*: 'Preparation of Y_2O_3 hollow nanospheres by homogeneous precipitation templates method', *Rare Met. Meter. Eng.*, 2014, **43**, (1), pp. 249–252

[11] Gaspar R.D.L., Mazali I.O., Sigoli F.A.: 'Particle size tailoring and luminescence of europium(III)-doped gadolinium oxide obtained by the modified homogeneous precipitation method: dielectric constant and counter anion effects', *Colloids Surf. A, Physicochem. Eng. Asp.*, 2010, **367**, (3), pp. 155–160

[12] Zhao J.B., Wu L.L., Zhang C.J., *ET AL.*: 'Highly efficient saturated visible up-conversion photoluminescent $Y_2O_3:Er^{3+}$ microspheres pumped with a 1.55 μm laser diode', *J. Mater. Chem. C*, 2017, **5**, pp. 3903–3907

[13] Borlaf M., Colomer M.T., Moreno R., *ET AL.*: 'Rare earth-doped TiO_2 nanocrystalline thin films: preparation and thermal stability', *J. Eur. Ceram. Soc.*, 2014, **34**, (16), pp. 4457–4462

[14] Yang W.J., Chang J.H.: 'Syntheses of colorless and transparent poly (ester imide)s and their PET blends: thermo-mechanical properties and optical transparency', *Polym. Korea*, 2016, **40**, (3), pp. 405–413

[15] Bunekar N., Tsai T.Y., Yu Y.Z.: 'Synthesis and characterization of Poly(ethylene terephthalate)/bio inorganic modified LiAl LDH nanocomposites', *Mater. Today*, 2016, **3**, (6), pp. 1415–1422

[16] Swar S., Zajicova V., Rysova M., *ET AL.*: 'Biocompatible surface modification of poly(ethylene terephthalate) focused on pathogenic bacteria: promising prospects in biomedical applications', *J. Appl. Polym. Sci.*, 2017, **134**, pp. 1–11

doi: 10.1049/mnl.2017.0570